Relationships between large-scale circulation patterns and carbon dioxide exchange by a deciduous forest

Jingyong Zhang,[1] Lingyun Wu,[1] Gang Huang,[2] and Michael Notaro[3]

Received 9 July 2010; revised 27 November 2010; accepted 14 December 2010; published 17 February 2011.

[1] In this study, we focus on a deciduous forest in central Massachusetts and investigate the relationships between global climate indices and CO_2 exchange using eddy-covariance flux measurements from 1992 to 2007. Results suggest that large-scale circulation patterns influence the annual CO_2 exchange in the forest through their effects on the local surface climate. Annual gross ecosystem exchange (GEE) in the forest is closely associated with spring El Niño–Southern Oscillation (ENSO) and Pacific Decadal Oscillation (PDO), previous fall Atlantic Multidecadal Oscillation (AMO), and previous winter East Pacific–North Pacific (EP-NP) pattern. Annual net ecosystem exchange (NEE) responds to previous fall AMO and PDO, while annual respiration (R) is impacted by previous fall ENSO and Pacific/North American Oscillation (PNA). Regressions based on these relationships are developed to simulate the annual GEE, NEE, and R. To avoid problems of multicollinearity, we compute a "Composite Index for GEE (CI_{GEE})" based on a linear combination of spring ENSO and PDO, fall AMO, and winter EP-NP and a "Composite Index for R (CI_R)" based on a linear combination of fall ENSO and PNA. CI_{GEE}, CI_R, and fall AMO and PDO can explain 41, 27, and 40% of the variance of the annual GEE, R, and NEE, respectively. We further apply the methodology to two other northern midlatitude forests and find that interannual variabilities in NEE of the two forests are largely controlled by large-scale circulation patterns. This study suggests that global climate indices provide the potential for predicting CO_2 exchange variability in the northern midlatitude forests.

Citation: Zhang, J., L. Wu, G. Huang, and M. Notaro (2011), Relationships between large-scale circulation patterns and carbon dioxide exchange by a deciduous forest, *J. Geophys. Res.*, *116*, D04102, doi:10.1029/2010JD014738.

1. Introduction

[2] The terrestrial ecosystem plays a dominant role in influencing interannual variability of the global carbon cycle, with major contributions from northern midlatitude forests [e.g., *Tans et al.*, 1990; *Keeling et al.*, 1996; *Battle et al.*, 2000; *Houghton*, 2000]. The interannual fluctuations of northern midlatitude forest CO_2 exchange have been found to be regulated by weather and seasonal climate variables such as surface air temperature, summertime solar radiation, and precipitation anomalies [e.g., *Graumlich et al.*, 1989; *Goulden et al.*, 1996; *Barford et al.*, 2001; *Dunn et al.*, 2007; *Wang et al.*, 2008].

[3] Recently, the eddy-covariance technique has emerged as a popular way to assess ecosystem CO_2 exchange because the technique can produce a direct and continuous measurement of net CO_2 exchange across the canopy-atmosphere interface [e.g., *Wofsy et al.*, 1993; *Baldocchi*, 2003]. At present, the lengthened eddy covariance data records of CO_2 exchange provide an excellent opportunity to explore the interannual variability of northern midlatitude forest CO_2 exchange. Harvard Forest AmeriFlux site is located in a mixed deciduous forest, northeast United States (Central Massachusetts), and is the longest running eddy flux site in the world. The site is typical of the northeast United States biomes [e.g., *Wofsy et al.*, 1993; *Goulden et al.*, 1996; *Ollinger et al.*, 2008a]. During the last 2 decades, CO_2 exchange between the atmosphere and Harvard Forest is the subject of much research [e.g., *Wofsy et al.*, 1993; *Goulden et al.*, 1996; *Barford et al.*, 2001; *Urbanski et al.*, 2007]. The net CO_2 exchange at the site has experienced distinct interannual variations [*Goulden et al.*, 1996; *Barford et al.*, 2001; *Urbanski et al.*, 2007]. While variations in CO_2 exchange at short-term scales (hourly to monthly) were simulated well as prompt responses to the weather patterns and local conditions at Harvard Forest [e.g., *Urbanski et al.*, 2007] and other northern midlatitude forests [e.g., *Hollinger et al.*, 1999], interannual variations and long-term trend in CO_2

[1]Center for Monsoon System Research, Institute of Atmospheric Physics, Chinese Academy of Sciences, Beijing, China.

[2]RCE-TEA and LASG, Institute of Atmospheric Physics, Chinese Academy of Sciences, Beijing, China.

[3]Center for Climatic Research, University of Wisconsin-Madison, Madison, Wisconsin, USA.

0148-0227/11/2010JD014738

exchange are often poorly represented by current models [*Hanson et al.*, 2004; *Siqueira et al.*, 2006; *Richardson et al.*, 2007; *Urbanski et al.*, 2007]. The annual CO_2 exchange at Harvard Forest have been found to be sensitive to climatic factors during and before the growing season [*Goulden et al.*, 1996; *Barford et al.*, 2001; *Urbanski et al.*, 2007]. The critical role of climatic factors in influencing the interannual variability of CO_2 exchange is also evident in other northern midlatitude forests [e.g., *Graumlich et al.*, 1989; *Houghton*, 2000; *Hui et al.*, 2003; *Dunn et al.*, 2007; *Wang et al.*, 2008].

[4] Large-scale circulation patterns influence the location and intensity of synoptic atmospheric pressure systems, and thereby significantly modify northern midlatitude climate [e.g., *Wallace and Gutzler*, 1981; *Barnston and Livezey*, 1987; *Hurrell*, 1995, 1996] and ecosystems [e.g., *Goldstein et al.*, 2000; *Freedman et al.*, 2001; *Morgenstern et al.*, 2004; *Urbanski et al.*, 2007; *Hember and Lafleur*, 2008; *Grant et al.*, 2009; *Wharton et al.*, 2009]. Over the northeast United States, previous studies have demonstrated that the climate and circulation features are strongly influenced by large-scale circulation patterns in the Pacific, Atlantic and Arctic regions. For example, there is evidence for significant teleconnections between the Pacific Decadal Oscillation (PDO), the Atlantic Multidecadal Oscillation (AMO), the Southern Oscillation, Pacific/North American Oscillation (PNA), and the North Atlantic Oscillation (NAO) and precipitation in the northeast United States [e.g., *Richman et al.*, 1991; *McCabe et al.*, 2004; *Notaro et al.*, 2006a]. The surface air temperatures in this region have also been reported to be closely correlated with PNA, the North Atlantic Oscillation (NAO), the Arctic Oscillation (AO), the Quasi-Biennial Oscillation (QBO), and the East Pacific–North Pacific (EP-NP) pattern [e.g., *Leathers et al.*, 1991; *Bradbury et al.*, 2002; *Thompson et al.*, 2002; *Budikova*, 2005; *Notaro et al.*, 2006a]. In addition, the El Niño–Southern Oscillation has been reported to affect drought and snowfall over the northeast United States [*Ropelewski and Halpert*, 1986; *Griffiths and Bradley*, 2007; *Kunkel et al.*, 2009].

[5] Considering the critical role of surface climate in influencing northern midlatitude forest CO_2 exchange, we, therefore, hypothesize that large-scale circulation patterns exert influence on CO_2 exchange at Harvard Forest and other sites through their effects on local climatic conditions. Moreover, the global climate indices may provide the potential for predicting forest CO_2 exchange. In this study, we take Harvard Forest AmeriFlux site with data records from 1992 to 2007 as an example to investigate the relationships between CO_2 exchange and large-scale circulation patterns, and develop empirical models based on these relationships to predict CO_2 exchange.

[6] This paper is organized as follows. The data and statistical methods are described in section 2. In section 3, we first examine the relationships among large-scale circulation patterns, surface climate, and CO_2 exchange at Harvard Forest. Then, we develop empirical models based on the relationships between large-scale circulation patterns and CO_2 exchange to predict CO_2 exchange at Harvard Forest. Also discussed in section 3 is the application of the methodology to other two AmeriFlux forest sites which both have more than 10 years of CO_2 flux records. Finally, the conclusions are given in section 4.

2. Data and Methods

2.1. CO_2 Fluxes and Meteorological Data

[7] Net ecosystem exchange (NEE) represents the net exchange of CO_2 between terrestrial ecosystems and the atmosphere [*Law*, 2006], gross ecosystem exchange (GEE) is photosynthetic CO_2 uptake, and R is the sum of heterotrophic (soil microorganisms) and autotrophic (plants) respiration. Continuous measurements of CO_2 flux and environmental variables are collected from online data information systems maintained by AmeriFlux (http://public.ornl.gov/ameriflux/). In this study we use NEE, R, and GEE data for 1992–2007 at Harvard Forest Environmental Monitoring Site, located on the Prospect Hill tract of Harvard Forest (42.54°N, 72.17°W, elevation 340 m a.s.l. (above sea level)) [*Wofsy et al.*, 1993; *Goulden et al.*, 1996] (also J. W. Munger and S. Wofsy, EMS - Canopy-Atmosphere Exchange of Carbon, Water and Energy, Harvard Forest Data Archive: HF004, 1999, http://harvardforest.fas.harvard.edu:8080/exist/xquery/data.xq?id=hf004; hereafter Munger and Wofsy, online archive, 1999). NEE was measured by using eddy-covariance technique and R was measured during dark periods and estimated as a function of soil temperature during light periods. GEE was computed from NEE-R (note that by convention, uptake of CO_2 from the atmosphere has negative sign so GEE < 0). The flux of photosynthetically active radiation (PAR) is radiation used by plants for photosynthesis and is important in evaluating the effect of light on plant growth. We use the measured PAR above the canopy (29 m) (Munger and Wofsy, online archive, 1999) to explore its effects on CO_2 exchange. Precipitation and temperature are obtained from Shaler Meteorological Station (1992–2001, Harvard Forest, 42.53°N, 72.19°W) (E. Boose and E. Gould, Shaler Meteorological Station (1964–2002), Harvard Forest Data Archive: HF000, 1999, http://harvardforest.fas.harvard.edu:8080/exist/xquery/data.xq?id=hf000), and Fisher Meteorological Station (2002–2007, Harvard Forest, 42.53°N, 72.19°W) (E. Boose, Fisher Meteorological Station (since 2001), Harvard Forest Data Archive: HF001, 2001, http://harvardforest.fas.harvard.edu:8080/exist/xquery/data.xq?id=hf001).

[8] We also use NEE data from Howland Forest and Morgan Monroe State Forest AmeriFlux research sites. The Howland Forest AmeriFlux research site is located about 35 miles north of Bangor, Maine, USA (45.20°N, 68.74°W, elevation 60 m a.s.l.), and has the data records from 1996 to 2008. The Morgan Monroe State Forest AmeriFlux research site is located in south-central Indiana (39.32°N, 86.41°W, elevation 275 m a.s.l.) with the data measurements from 1998 to 2008.

[9] Table 1 describes the characteristics of the three sites. It is worthwhile to note that the three forests have different dominant species composition. Harvard Forest and Morgan Monroe State Forest are located in mixed temperate forests dominated by deciduous species, while Howland Forest is located in a boreal northern hardwood transition forest with predominantly evergreen species. Previous studies have shown that the forest species can influence carbon uptake. For example, *Hollinger et al.* [1999] demonstrated that the

Table 1. Site Descriptions Including Name and Location, Latitude, Longitude, Canopy Height, Time Span, Stand Age, Dominant Species Composition, and References for Each Flux Site in the Analysis

Site Name and Location	Latitude (deg)	Longitude (deg)	Canopy Height (m)	Time Span	Stand Age (years)	Dominant Species Composition	References
Harvard Forest (MA, USA)	42.54	−72.17	23	1992–2007	70–110	Temperate deciduous forest dominated by red oak, red maple, black birch, white pine, and hemlock	*Urbanski et al.* [2007]
Howland Forest Main (ME, USA)	45.20	−68.74	20	1996–2008	60–190	Conifer forest dominated by red spruce, eastern hemlock, other conifers, and hardwoods	*Hollinger et al.* [1999, 2004]
Morgan Monroe State Forest (IN, USA)	39.32	−86.41	27	1998–2008	60–80	Mixed hardwood deciduous forest dominated by sugar maple, tulip poplar, sassafras, white oak, and black oak	*Schmid et al.* [2000]

evergreen forest at Howland has longer growing season, while deciduous forest at Harvard has greater maximum rates of carbon uptake in midsummer.

2.2. Large-Scale Circulation Patterns

[10] Global climate indices used in this study include AMO, AO, EP-NP, Multivariate El Niño–Southern Oscillation Index (MEI), NAO, PDO, PNA, and QBO. The methodologies and characteristics of the global climate indices are listed in Table 2. All indices are obtained from http://www.esrl.noaa.gov/psd/data/climateindices/list/. Fall indices are defined from September to November of the prior year. Winter indices are defined from December of the prior year through February of the listed year. Since there are no records of EP-NP in December (the pattern of EP-NP is not a leading mode in December), we average January and February to calculate the winter EP-NP index. Spring and summer indices are computed based on March–May and June–August values, respectively.

2.3. Statistical Methods

[11] Since Spearman's rank correlation is nonparametric and insensitive to extreme values such as those commonly encountered in meteorological time series, it is a useful method to test for monotonic relationships [*Sobolowski and Frei*, 2007]. We first calculate Spearman's rank correlation coefficients (r) to examine associations between the global climate indices and annual CO_2 exchange at Harvard forest.

[12] Composite analyses are then applied to the 5 strongest and 5 weakest years of specific global climate indices which show significant ($p \leq 0.05$) correlations with the annual GEE, NEE, and R at Harvard Forest. If both the correlation and composite difference are significant at the 95% confidence level, the relationship is thought to be robust in this study. Spearman's rank correlation and composite analysis are also applied to examine the relationships between large-scale circulation patterns and surface climate, and between surface climate and CO_2 exchange. Finally, regressions based on these global climate indices which have robust relationships with the annual GEE, NEE, and R are developed to simulate their interannual variations. The methodology is also applied to Howland Forest and Morgan Monroe State Forest AmeriFlux research sites which both have more than 10 years of CO_2 flux records to test its applicability to other sites.

3. Results

3.1. Relationships Between Climatic Indices and CO_2 Fluxes

[13] Figure 1 shows Spearman's rank correlation coefficients between the annual GEE, NEE and R and the seasonal climate indices. The annual GEE is significantly and positively correlated with spring MEI (r = 0.66, p < 0.01) and PDO (r = 0.52, p < 0.04), and winter EP-NP (r = 0.52, p < 0.05), while showing a significant anticorrelation with fall (r = −0.58, p < 0.03) and winter (r = −0.52, p < 0.05) AMO. Fall (r = −0.58, p < 0.03) and winter (r = −0.52, p < 0.05) AMO are also found to inversely vary with the annual NEE. Additionally, the annual NEE is negatively correlated with fall AO (r = −0.57, p < 0.03), and is positively correlated with fall EP-NP (r = 0.54, p < 0.04) and PDO (r = 0.52, p < 0.04). The relationships imply that during the period of 1992–2007, more negative NEE anomalies are most often associated with warm phases of fall and winter AMO and fall AO and with cool phases of fall EP-NP and PDO. The annual R is observed to be positively correlated to fall PNA (r = 0.55, p < 0.03), but is inversely correlated to spring PNA (r = −0.64, p < 0.01). Another global climate index inversely related to the annual R is fall MEI (r = −0.59, p < 0.02). The annual GEE, NEE and R do not exhibit any statistically significant relationships with summer climate indices because large-scale circulation patterns/teleconnections are typically weak during summer. It is interesting to note that the Pacific teleconnections are important for R (MEI, PNA), while both the Pacific and Atlantic teleconnections affect NEE and GEE.

[14] The composite analysis is further applied to test the relationships of the annual GEE, NEE, and R to global climate indices identified in the correlation analysis. Table 3 presents composite differences in the annual GEE, NEE and R between 5 strongest and 5 weakest years of global climate indices. The composite annual GEE exhibits a significant lower-than-normal value corresponding to a strong spring MEI, spring PDO, winter EP-NP, or a weak fall AMO situation. The weak spring MEI, spring PDO, winter EP-NP,

Table 2. Methodology, Characteristics, and References for Global Climate Indices Used in the Study

Name	Definition	Characteristics	Data Source[a]	References
AO (Arctic Oscillation)	Leading principal component (PC) of monthly mean sea level pressure (SLP) in Northern Hemisphere (poleward of 20°N)	The oscillation exhibits a "negative phase" with relatively low pressure at the midlatitude (about 45°N), and a "positive phase" in which the pattern is reversed.	CPC	*Thompson and Wallace* [1998]
AMO (Atlantic Multidecadal Oscillation)	Detrended sea surface temperature (SST) anomalies averaged over the North Atlantic from 0 to 70°N	AMO-like variability is associated with small changes in the North Atlantic branch of the Thermohaline Circulation.	PSD	*Enfield et al.* [2001]
EP-NP (East Pacific–North Pacific Pattern)	Orthogonally rotated (10 varimax rotations) principal component analysis (RPCA) of the Northern Hemisphere monthly mean height anomalies at 700 hPa	EP-NP pattern is a spring-summer-fall pattern with three main anomaly centers. The positive phase of this pattern is associated with above-average surface temperatures over the eastern North America.	CPC	*Barnston and Livezey* [1987], *Bell and Janowiak* [1995]
MEI (Multivariate ENSO Index)	First unrotated PC of six observed variables (SLP, zonal and meridional component of surface wind, SST, surface air temperature, total cloudiness fraction) over the tropical Pacific	ENSO typically transitions from a warm phase (El Niño) to a cool phase (La Niña) every 2–7 years in the equatorial Pacific Ocean.	PSD	*Wolter and Timlin* [1993, 1998]
NAO (North Atlantic Oscillation)	The first leading mode of Rotated Empirical Orthogonal Function (REOF) analysis of monthly mean 500 mb height during 1950–2000 period	NAO is a largely atmospheric mode. It is one of the most important manifestations of climate fluctuations in the North Atlantic and surrounding humid climates. During the winter, when the index is high (NAO+), the Icelandic low draws a stronger southwesterly circulation over the eastern half of the North American continent which prevents Arctic air from plunging southward.	CPC	*Hurrell* [1995]
PDO (Pacific Decadal Oscillation)	Leading PC from an unrotated EOF analysis of monthly residual North Pacific SST anomalies	SST normally remains consistently above or below the long-term average for two to three decades. The climatic fingerprints of the PDO were most visible in the North Pacific/North American sector.	PSD	*Mantua et al.* [1997]
PNA (Pacific North American Index)	Leading eigenvector from a rotated PCA based on the 700 hPa height field in the North Pacific	A major mode of atmospheric variability North America during the Northern Hemisphere winter. The index is a function of the phase and intensity of quasi stationary Rossby waves over North America and a good indicator of the mean location of the polar front jet during colder months.	CPC	*Wallace and Gutzler* [1981]
QBO (Quasi-Biennial Oscillation)	Zonal average of the 30 mbar zonal wind at the equator	The QBO is a quasiperiodic oscillation of the equatorial zonal wind between easterlies and westerlies in the tropical stratosphere with a mean period of 28 to 29 months.	PSD	*Holton and Lindzen* [1972]

[a]CPC, NOAA Climate Prediction Center; PSD, NOAA Physical Sciences Division.

or strong fall AMO phase brings an opposite change to the annual GEE. However, the annual GEE does not exhibit significant difference between 5 strongest and 5 weakest years of the winter AMO. This suggests that the relationship between the annual GEE and the winter AMO is not robust. We therefore drop the winter AMO, and only use the other four global climate indices in the following regression analysis for the annual GEE. For the annual NEE, both correlation and composite analyses show that it is closely related with the fall AMO and PDO. However, composite differences are not significant for the winter AMO, and fall AO and EP-NP. Therefore, the three climate indices are not

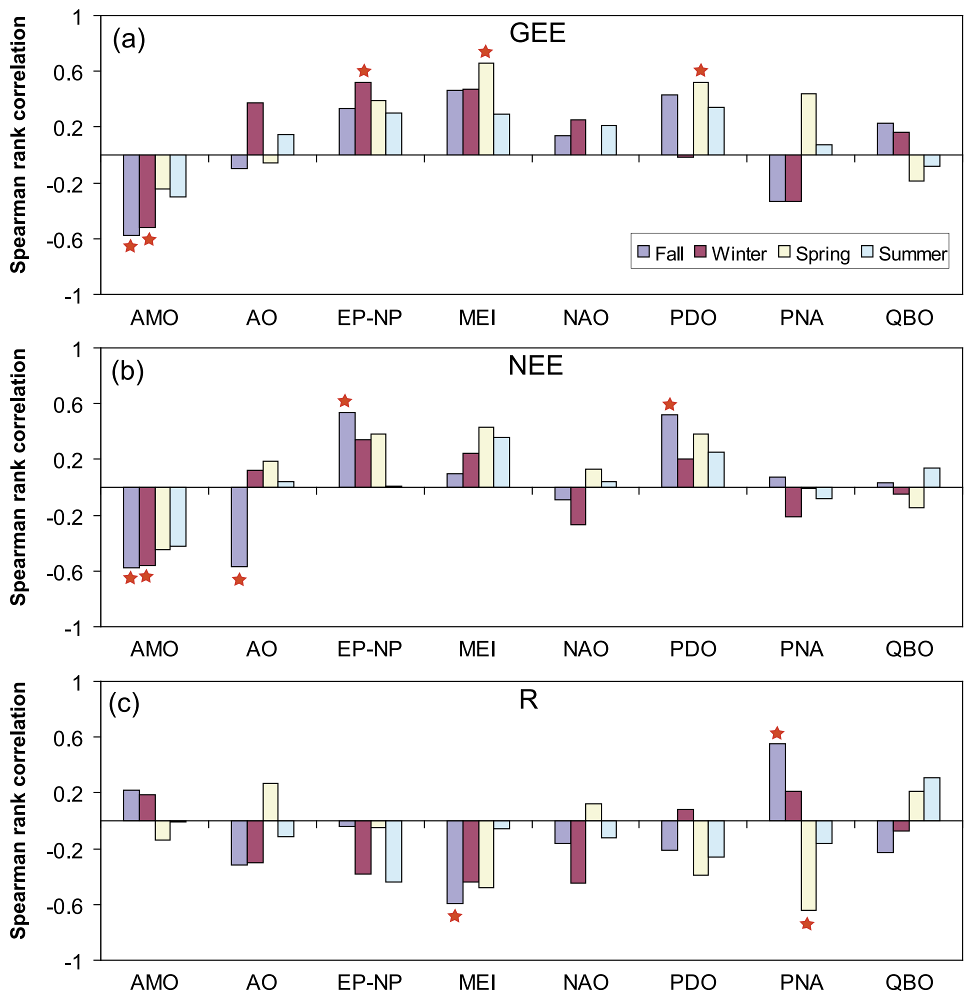

Figure 1. Spearman's rank correlation coefficients between seasonal climate indices and (a) annual gross ecosystem exchange (GEE), (b) annual net ecosystem exchange (NEE), and (c) annual respiration (R) at Harvard Forest. Orange stars represent that the correlations are significant at the 95% confidence level.

Table 3. Composite Analysis of CO_2 Exchange Between Five Strongest and Five Weakest Index Years[a]

	Strongest Mean (μ mol m^{-2} s^{-1})	Weakest Mean (μ mol m^{-2} s^{-1})	Difference (μ mol m^{-2} s^{-1})
		GEE	
Fall AMO	−4.22 (1999, 2002, 2004, 2006, 2007)	−3.41 (1992, 1993, 1994, 1995, 1997)	−0.81[b]
Winter AMO	−3.96 (1999, 2000, 2005, 2006, 2007)	−3.64 (1992, 1993, 1994, 1998, 2001)	−0.32
Winter EP/NP	−3.59 (1993, 1994, 1995, 1996, 2003)	−4.13 (1999, 2000, 2001, 2002, 2006)	0.54[b]
Spring MEI	−3.37 (1992, 1993, 1995, 1998, 2005)	−4.02 (1996, 1999, 2000, 2001, 2006)	0.65[b]
Spring PDO	−3.62 (1993, 1996, 1998, 2003, 2005)	−4.11 (1999, 2000, 2001, 2002, 2007)	0.49[b]
		NEE	
Fall AMO	−1.03 (1999, 2002, 2004, 2006, 2007)	−0.51 (1992, 1993, 1994, 1995, 1997)	−0.52[b]
Winter AMO	−1.03 (1999, 2000, 2005, 2006, 2007)	−0.58 (1992, 1993, 1994, 1998, 2001)	−0.45
Fall AO	−0.96 (1999, 2001, 2002, 2004, 2005)	−0.62 (1995, 1996, 1998, 2003, 2007)	−0.34
Fall EP−NP	−0.68 (1992, 1993, 1994, 2000, 2007)	−1.03 (1995, 1997, 1998, 2002, 2004)	0.26
Fall PDO	−0.46 (1994, 1995, 1998, 2002, 2007)	−0.79 (1992, 1993, 1996, 1999, 2000)	0.33[b]
		R	
Fall MEI	2.77 (1995, 1996, 1998, 2000, 2004)	3.23 (2001, 2002, 2003, 2005, 2006)	−0.47[b]
Fall PNA	3.31 (1992, 1995, 1997, 2004, 2007)	2.76 (1996, 1999, 2000, 2001, 2002)	0.55[b]
Spring PNA	2.80 (1995, 1996, 2002, 2006, 2007)	3.28 (1992, 1993, 1994, 1997, 2004)	−0.48

[a]Strongest mean: the mean of GEE, NEE, and R in 5 strongest index years. Weakest mean: the mean of GEE, NEE, and R in 5 weakest index years. Difference: composite difference between the mean of GEE, NEE, and R in 5 strongest and 5 weakest index years (i.e., strong minus weak index years).
[b]Values represent that differences between strongest and weakest mean are significant at the >95% confidence level tested by Student's *t* test.

Table 4. Spearman's Rank Correlation Coefficients, and *p* Values, Between Temperature and Annual Net Ecosystem Exchange (NEE), Gross Ecosystem Exchange (GEE), and Respiration (R) During the Period of 1992–2007[a]

	Spring $_{max}$	Spring $_{min}$	Spring	Summer $_{max}$	Summer $_{min}$	Summer	Fall $_{max}$	Fall $_{min}$	Fall
NEE	−0.11 (0.68)	**−0.50 (0.05)**	−0.26 (0.32)	−0.04 (0.90)	**−0.6 (0.02)**	−0.14 (0.59)	**−0.51 (0.05)**	**−0.73 (0.01)**	**−0.71 (0.01)**
GEE	−0.11 (0.69)	**−0.48 (0.06)**	−0.27 (0.30)	0.05 (0.84)	**−0.7 (0.01)**	−0.21 (0.42)	−0.31 (0.24)	**−0.71 (0.01)**	**−0.44 (0.09)**
R	0.02 (0.95)	0.05 (0.85)	−0.01 (0.99)	−0.05 (0.85)	0.36 (0.17)	0.11 (0.67)	−0.02 (0.93)	0.32 (0.22)	0.02 (0.96)

[a]Spring $_{max}$ and Spring $_{min}$ represent the maximum and minimum surface air temperature in spring, respectively. Summer $_{max}$ and Summer $_{min}$ represent the maximum and minimum surface air temperature in summer, respectively. Fall $_{max}$ and Fall $_{min}$ represent the maximum and minimum surface air temperature in fall, respectively. Bold values denote that correlations are significant at the >90% confidence level.

used to regress the annual NEE. Similarly, we retain the fall MEI and PNA, but remove the spring PNA for regressing the annual R. The analysis implies that for the annual GEE, the large-scale circulation patterns are important for all seasons except summer, but for the annual NEE and R, only the fall large-scale circulation patterns are significant.

3.2. Relationships Between Large-Scale Circulation Patterns and Surface Climate

[15] We first examine regional atmospheric circulation and surface climate features associated with the global climate indices which have significant correlations with the annual GEE, NEE, and R (see the auxiliary material).[1] The results suggest that these global climate indices can modify regional atmospheric circulation patterns, thus influencing New England surface climate and ecosystems. We further examine the relationships between these global climate indices and several key climate factors that control interannual variability of the CO_2 exchange at Harvard Forest. Fall AMO can modify fall mean daily maximum ($r = 0.53$, $p < 0.04$), minimum ($r = 0.8$, $p < 0.002$) and average ($r = 0.67$, $p < 0.01$) temperatures at Harvard Forest. Additionally, the fall AMO is found to influence the annual mean daily minimum temperature ($r = 0.64$, $p < 0.01$) and fall precipitation ($r = 0.55$, $p < 0.03$). Spring MEI is suggested to influence the fall mean daily minimum temperature ($r = -0.39$, $p < 0.13$) to some degree. In addition, the fall PNA is found to be linked to spring mean daily maximum temperature ($r = 0.36$, $p < 0.16$).

[16] The negative (positive) phase of the winter EP-NP pattern which is associated with an enhanced cyclonic (anticyclonic) circulation over the northeast United States, is followed by smaller (larger) winter precipitation ($r = 0.52$, $p < 0.05$) at Harvard Forest. Fall PDO ($r = 0.60$, $p < 0.02$) and MEI ($r = 0.42$, $p < 0.10$) are positively correlated with winter precipitation. In addition, significant correlations between the spring PDO ($r = -0.65$, $p < 0.01$) and the fall AMO ($r = 0.54$, $p < 0.04$) and the annual PAR at Harvard Forest suggest that the two climate indices can largely influence the PAR. In section 3.3, we further look at how the surface climate affects CO_2 exchange at Harvard Forest.

3.3. Relationships Between Surface Climate and CO_2 Exchange

[17] Temperature, water, and radiation are main abiotic controls of CO_2 exchange [*Boisvenue and Running*, 2006]. Table 4 shows Spearman's rank correlations between temperature and the annual NEE, GEE, and R at Harvard Forest. The annual NEE and GEE are sensitive to spring and summer mean daily minimum temperatures, and fall mean daily maximum, minimum and average temperatures. *Goulden et al.* [1996] demonstrated that large changes in the annual GEE are associated with modest changes in the length of the growing season. The length of the growing season is linked to the timing of leaf expansion and senescence, which is regulated by surface air temperature in spring and fall [e.g., *Goulden et al.*, 1996; *Piao et al.*, 2008]. It is noted that the minimum air temperatures during spring, summer, fall and the growing season play a critical role in controlling the annual GEE and NEE at Harvard Forest. In addition, the CO_2 uptake at Harvard Forest is particularly sensitive to fall air temperatures. Fall temperature has significantly increased (13.37%) since 1999, whereas spring (5.60%) and summer (6.45%) air temperatures experienced relatively smaller increases. The fall warming could subsequently enhance CO_2 uptake (the annual GEE and NEE have increased 21.54 and 103.98%, respectively, since 1999) by a longer growing season and greater photosynthetic activity [*Zhou et al.*, 2001; *Churkina et al.*, 2005]. On the other hand, Table 4 shows that the annual R is partly controlled by summer mean daily minimum temperature ($r = 0.36$, $p < 0.17$).

[18] Previous studies have found that the annual gross CO_2 uptake at Harvard Forest is particularly sensitive to the snow, rather than the annual precipitation [e.g., *Goulden et al.*, 1996]. Since we only have snow depth records from 1992 to 2001 available, instead we use the averaged winter (November through March) precipitation records from 1992 to 2007 to explore the snow cover–CO_2 exchange link. Table 5 shows Spearman's rank correlations between seasonal precipitation and the annual NEE, GEE, and R at Harvard Forest. The results show that the winter precipitation is positively correlated with the annual GEE and NEE, and negatively correlated with the annual R. Spring and summer precipitation generally have small effects on the annual GEE, NEE and R.

[19] All biological activity in plants is ultimately dependent on absorbed solar radiation, even though the solar radiation alone does not determine the primary productivity [*Boisvenue and Running*, 2006]. The PAR is radiation used by plant for photosynthesis and is important in evaluating the effect of light on plant growth. The GEE is widely noted to increase systematically with incident PAR, and thus is usually specified as a function of PAR [e.g., *Wofsy et al.*, 1993; *Xiao et al.*, 2004]. During the study period, the annual NEE and GEE are found to generally have significant and negative correlations with spring, summer, fall, and the entire growing season PAR, indicating that the higher PAR favors more NEE and GEE (Table 6; note that by convention, uptake of CO_2 from the atmosphere has negative sign

[1]Auxiliary materials are available in the HTML: doi:10.1029/2010JD014738.

Table 5. Spearman's Rank Correlation Coefficients, and *p* Values, Between Precipitation and Annual Net Ecosystem Exchange (NEE), Gross Ecosystem Exchange (GEE), and Respiration (R) During the Period of 1992–2007[a]

	Winter (Nov–Mar)	Spring (Apr–May)	Summer (Jun–Aug)	Fall (Sep–Oct)
NEE	**0.66 (0.01)**	−0.38 (0.14)	−0.18 (0.48)	**−0.52 (0.04)**
GEE	**0.69 (0.01)**	−0.36 (0.16)	0.02 (0.96)	0.17 (0.51)
R	−0.39 (0.13)	0.14 (0.60)	−0.21 (0.43)	−0.13 (0.62)

[a]Winter precipitation is defined from November of the prior year through March of the listed year. Bold values denote that correlations are significant at the >90% confidence level.

in this study). This conclusion is in agreement with that from previous studies.

[20] This study identifies the statistical relationships between CO_2 exchange and global climate indices, and discusses possible physical processes linking these phenomena. However, we realize that a comprehensive understanding of the physical mechanisms involved is impossibly reached through the statistical analysis. Further investigations are clearly needed to clarify the related physical mechanisms.

3.4. Regression Analysis

[21] Regressions based on these global climate indices which have robust relationships with the annual GEE, NEE, and R are developed to simulate their interannual variations. However, during the study period, the four global climate indices of spring MEI and PDO, fall AMO and winter EP-NP, all of which impact the annual GEE are highly correlated to one another (Table 7). Also, the two indices of fall MEI and PNA, associated with the annual R, are highly correlated to each other ($r = -0.51$, $p \le 0.05$). We therefore use a regression analysis called principal components analysis (PCA) to avoid problems of multicollinearity [*Kutner et al.*, 2004]. For the annual GEE, instead of regressing highly correlated PDO, MEI, AMO and EP-NP directly, we calculate four principal components which are uncorrelated, each component being a linear combination of the correlated four climate indices. The first principal component (PC-1) explains 69.41% of the total variance in the four indices. We use the broken-stick distribution to evaluate the significance of the PC-1, whose criterion is one of the most reliable to check the significance of PCA axes [e.g., *Peres-Neto et al.*, 2003]. The broken-stick method is based on eigenvalues from random data, and assumes that if the total variance (i.e., sum of the eigenvalues) is divided randomly among the various components, then the expected distribution of the eigenvalues will follow a broken-stick distribution [*Frontier*, 1976; *Jackson*, 1993]. Result shows that the PC-1 with a larger percentage of variance than the broken-stick variance (52.08%) is significant [*Legendre and Legendre*, 1998]. Therefore, we select the PC-1 as a new index called the "Composite Index for GEE" (CI_{GEE}) to represent changes in the four climate indices. Similarly, for R, the first principal component (PC-1) explains 77.19% of the total variance in the fall AMO and PNA, which is larger than the broken-stick variance (75%). We select the PC-1 as another new index called the "Composite Index for R" (CI_R) to represent changes in the two climate indices. The PCA is not applied to the fall AMO and PDO associated with the annual NEE since they are not significantly correlated to each other ($r = -0.31$, $p < 0.23$). Instead, we directly regress the two climate indices to simulate the annual NEE.

Table 6. Spearman's Rank Correlation Coefficients, and *p* Values, Between Photosynthetically Active Radiation (PAR) and Annual Net Ecosystem Exchange (NEE), Gross Ecosystem Exchange (GEE), and Respiration (R) During the Period of 1992–2007[a]

	Spring (Apr–May)	Summer (Jun–Aug)	Fall (Sep–Oct)	Growing Season
NEE	**−0.45 (0.08)**	**−0.44 (0.09)**	**−0.43 (0.10)**	**−0.47 (0.07)**
GEE	−0.35 (0.18)	**−0.49 (0.06)**	**−0.55 (0.04)**	**−0.47 (0.07)**
R	0.07 (0.78)	0.32 (0.21)	0.25 (0.33)	0.10 (0.72)

[a]Bold values denote that correlations are significant at the >90% confidence level.

[22] Figure 2 shows that CI_{GEE} is highly correlated with the fall AMO ($R^2 = 0.39$), the winter EP-NP ($R^2 = 0.55$), and the spring MEI ($R^2 = 0.78$) and PDO ($R^2 = 0.71$). Winter EP-NP, spring MEI and PDO and CI_{GEE} are found to mostly have the same signs, and fall AMO and CI_{GEE} mostly have the opposite signs (Table 8). Those indicate that the new index is a well-defined property of the four climate indices. Table 9 shows that changes of CI_R and fall MEI are completely in phase. CI_R exhibits a very high correlation with the fall MEI ($R^2 = 0.97$), while it has a much weaker but still significant ($R^2 = 0.27$, $p < 0.05$) relationship with the fall PNA. Here we develop empirical prediction models to predict the annual mean GEE, NEE and R based on CI_{GEE}, fall AMO and PDO, and CI_R using linear regressions for the period of 1992–2007,

$$GEE = -3.82 + 0.27CI_{GEE}, \tag{1}$$

$$NEE = -0.65 - 0.94AMO_{fall} + 0.06PDO_{fall}, \tag{2}$$

$$R = 3.05 - 0.21CI_R. \tag{3}$$

Figure 3 shows the observed and predicted annual GEE, NEE, and R at Harvard Forest for the period of 1992 to 2007. The prediction of annual NEE is based on the fall AMO and PDO, while the prediction of annual GEE and annual R are based on CI_{GEE} and CI_R, respectively. Using a terrestrial ecosystem model (IBIS2), *Urbanski et al.* [2007] found that the decadal trend in the interannual variations of NEE and GEE cannot be predicted well. In this study, the CI_{GEE} can

Table 7. Correlation Coefficients, and *p* Values, of the Four Climate Indices Linked to Annual Gross Ecosystem Exchange (GEE)

	Fall AMO	Winter EP-NP	Spring MEI	Spring PDO
Fall AMO	1			
Winter EP-NP	−0.58 (0.03)	1		
Spring MEI	−0.52 (0.04)	0.62 (0.02)	1	
Spring PDO	−0.44 (0.09)	0.77 (0.003)	0.58 (0.03)	1

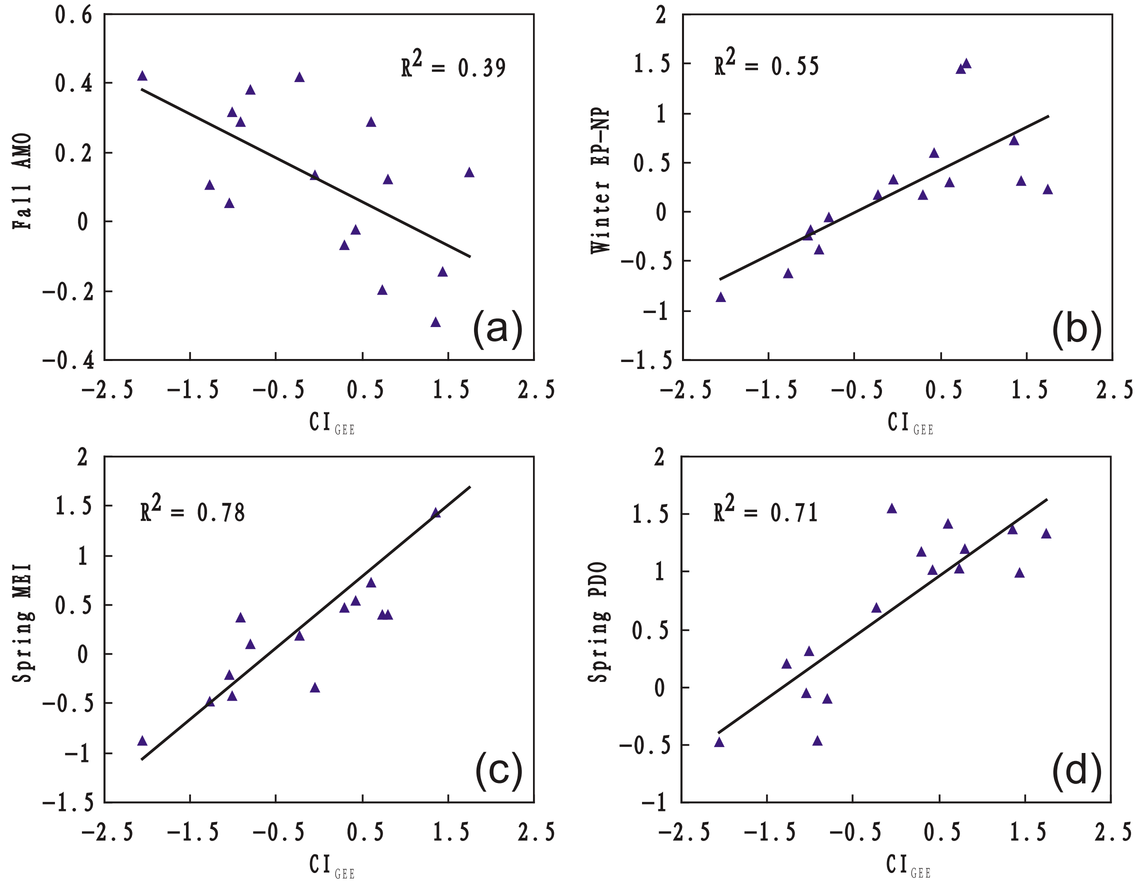

Figure 2. The relationship between "Composite Index for GEE (CI_{GEE})" and (a) fall AMO, (b) winter EP-NP, (c) spring MEI, and (d) spring PDO. CI_{GEE} is a linear combination of the four global climate indices.

simulate the interannual variability of the annual GEE to a large degree, explaining 41% of the total variance. Moreover, it can capture the observed decadal change. From 1992 through 1998, CI_{GEE} are mostly in positive phases with corresponding smaller annual GEE. Since 1999, CI_{GEE} are mostly in negative phases and associated with increased GEE compared to the 1992–1998 average (Table 8). Should current negative CI_{GEE} conditions persist into the upcoming decade, we suggest that higher GEE at Harvard Forest will continue compared with the 1992–1998 average. Forty percent of the variance of the annual NEE can be captured by the fall AMO and PDO. Also, consistent decadal changes in both observed and predicted annual NEE are demonstrated. These results suggest that the two climate indices can play an important role in influencing both interannual variability and decadal change of the annual NEE. The CI_R accounts for 27% of the variance of the annual R, which is lower relative to the explained variances of the annual GEE and NEE by CI_{GEE}, and the fall AMO and PDO. Further analysis indicates that the annual R varies consistently with CI_R before 2001. However, since then, changes of observed and predicted annual R appear, to a large extent, to be out of phase. Therefore, we split the annual R time series into two groups (1992 to 2000 and 2001 to 2007), and then examine their relationships with CI_R (Figure 4). CI_R exhibits a strong relationship with annual R (R^2 = 0.59) during the period of 1992 to 2000. In contrast, it poorly captures the observed annual R (R^2 = 0.19) during the period of 2001 to 2007. This reason leading the relative weak dependence of annual R on the CI_R since 2001 is still unclear, and needs to be further investigated.

Table 8. The Phase Signs of Fall AMO, Winter EP-NP, Spring MEI and PDO, and CI_{GEE}, and the Frequency of Same and Opposite Signs of Two Climate Indices and CI_{GEE} During 1992 to 2007[a]

	1992	1993	1994	1995	1996	1997	1998	1999	2000	2001	2002	2003	2004	2005	2006	2007	Frequency
Fall AMO	−[a]	−[a]	−[a]	−[a]	+[a]	−[a]	+	+[a]	+[a]	+[a]	+[a]	+	+[a]	+	+[a]	+[a]	13 (81.25%)
Winter EP−NP	+[b]	+[b]	+[b]	+[b]	+	+[b]	+[b]	−[b]	−[b]	−[b]	−[b]	+[b]	+	+[b]	−[b]	−[b]	14 (87.50%)
Spring MEI	+[b]	+[b]	+[b]	+[b]	−[b]	+[b]	+[b]	−[b]	−[b]	−[b]	+	+[b]	+	+[b]	−[b]	+	13 (81.25%)
Spring PDO	+[b]	+[b]	+[b]	+[b]	+	+[b]	+[b]	−[b]	+	−[b]	−[b]	+[b]	+	+[b]	+	−[b]	12 (75%)
CI_{GEE}	+	+	+	+	−	+	+	−	−	−	−	+	−	+	−	−	

[a]The climate index and CI_{GEE} have opposite signs.
[b]The climate index and CI_{GEE} have same signs.

Table 9. The Phase Signs of Fall MEI and PNA and CI_R, and the Frequency of Same and Opposite Signs of Two Climate Indices and CI_R During 1992 to 2007[a]

	1992	1993	1994	1995	1996	1997	1998	1999	2000	2001	2002	2003	2004	2005	2006	2007	Frequency
Fall MEI	+[a]	+[a]	+[a]	+[a]	–[a]	–[a]	+[a]	–[a]	–[a]	–[a]	–[a]	+[a]	+[a]	+[a]	–[a]	+[a]	16 (100%)
Fall PNA	–[b]	–[b]	–[b]	–[b]	+[b]	–	+	+[b]	+[b]	–	+[b]	+	+	–[b]	+[b]	–[b]	11 (68.75%)
CI_R	+	+	+	+	–	–	+	–	–	–	–	+	+	+	–	+	

[a]The climate index and CI_R have same signs.
[b]The climate index and CI_R have opposite signs.

[23] This study demonstrates that large-scale circulation patterns play an important role in influencing interannual variability of GEE, NEE, and R at Harvard Forest, accounting for 27–41% of the total variances. In addition to the large-scale circulation patterns, the surface climate in the northeast United States can also be affected by other processes. For example, land-atmosphere interactions can exert impacts on the interannual surface climate variability in the northeast United States [e.g., *Freedman et al.*, 2001; *Notaro et al.*, 2006b; *Zhang et al.*, 2008], thus affecting the interannual variability of CO_2 exchange at Harvard Forest. In addition to the climate-related factors, other possible factors for the interannual variability of CO_2 exchange at Harvard Forest include CO_2 fertilization, nitrogen deposition, forest composition species, and disturbance (e.g., forest regrowth, forest harvesting and pets and fire suppression) [e.g., *Houghton et al.*, 1999; *Caspersen et al.*, 2000; *Schimel et al.*, 2000, 2001; *Albani et al.*, 2006; *Ollinger et al.*, 2008a]. Previous studies have shown that CO_2 fertilization has a significant impact on rates of CO_2 uptake at Harvard Forest [e.g., *Albani et al.*, 2006; *Ollinger et al.*, 2008b]. Nitrogen as a regulator of C assimilation is well established, and the availability of nitrogen may play a role in influencing interannual variability of CO_2 exchange at Harvard Forest [e.g., *Aber et al.*, 1998; *Ollinger et al.*, 2008a]. Moreover, some studies attribute changes in CO_2 exchange at Harvard Forest in part to increased dominance of red oak, which has a higher photosynthetic efficiency compared to red maple, and development of denser canopy and increased nutrient uptake due to warmer early spring periods, contributing to an increase in maximum photosynthetic rates in midsummer [*Urbanski et al.*, 2007; *Munger*, 2009].

3.5. Application of the Methodology to Other Sites

[24] In sections 3.1–3.4, CO_2 exchange at Harvard Forest is found to be closely linked to the large-scale circulation patterns, and we further develop the empirical prediction models to predict GEE, NEE, and R based on their relationships with global climate indices. In this section, we further test the applicability of the methodology using long-term measurements of CO_2 exchange at other two sites: Howland Forest and Morgan Monroe AmeriFlux research sites. We choose the two sites for the present analysis because they both have gap-filled CO_2 flux data covering more than

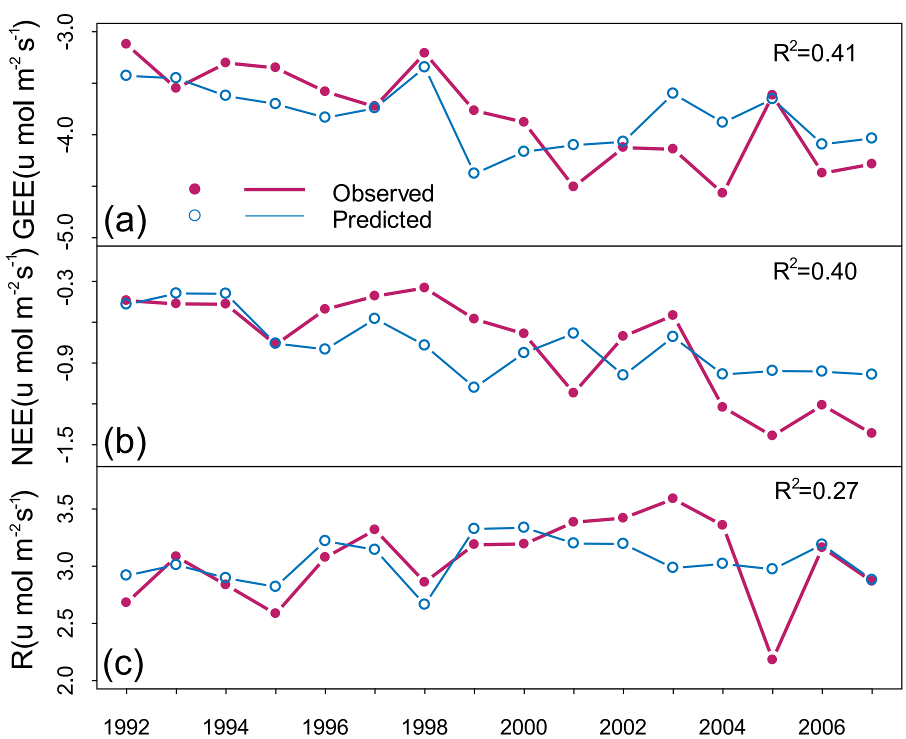

Figure 3. Observed and predicted (a) annual gross ecosystem exchange (GEE), (b) annual net ecosystem exchange (NEE), and (c) annual respiration (R) at Harvard Forest.

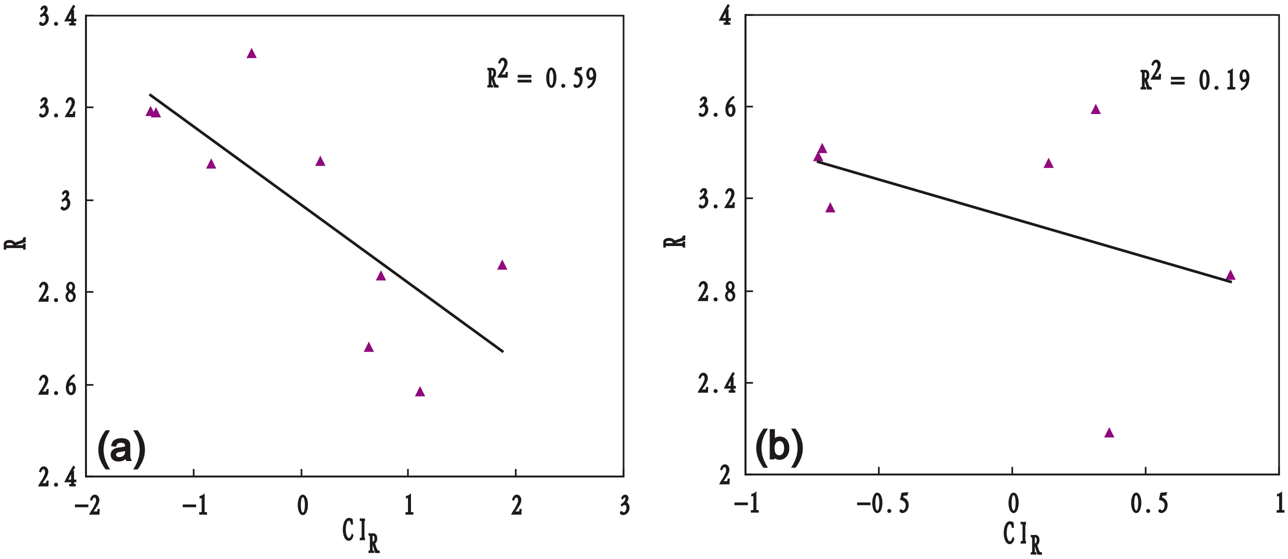

Figure 4. Scatterplots of annual respiration (R, μmol m^{-2} s^{1}) and "Composite Index for Respiration" (CI_R) during the period of (a) 1992 to 2000 and (b) 2001 to 2007.

10 years. Here, we focus on the relationships between large-scale circulation patterns and the annual NEE.

[25] The annual NEE at Howland Forest is inversely correlated with winter NAO ($r = -0.69$, $p < 0.02$), spring AMO ($r = -0.54$, $p < 0.06$) and PNA ($r = -0.49$, $p < 0.09$). The three global climate indices are not significantly correlated to one another, we therefore develop an empirical model based on the indices to predict the annual NEE using a linear regression,

$$NEE = -0.58 - 0.16NAO_{winter} - 0.25AMO_{spring} - 0.07PNA_{spring}. \quad (4)$$

Figure 5 shows the observed and predicted annual NEE at Howland Forest for the period of 1996 to 2008. More than half (55%) of the variance in the annual NEE is attributable to the three global climate indices.

[26] The annual NEE at Morgan Monroe State Forest is negatively correlated with fall and winter (September through February) AMO ($r = -0.67$, $p < 0.03$), and fall AO ($r = -0.53$, $p < 0.10$). The two indices are not significantly correlated ($r = 0.25$, $p < 0.45$). The empirical model based on the two indices using a linear regression to predict the annual NEE is as follows:

$$NEE = -0.82 - 0.70AMO_{fall-winter} - 0.11AO_{fall}. \quad (5)$$

Figure 6 shows the observed and predicted NEE at Morgan Monroe State Forest during 1998 to 2008. The two indices can simulate the interannual variability of the annual NEE well, together explaining 58% of the total variance.

[27] The above results show that global climate indices account for more than half of the total NEE variances at Howland Forest and Morgan Monroe State Forest, indicating that large-scale circulation patterns play a leading role in influencing the interannual variability of the annual NEE at the two forests. Combined with the results from Harvard Forest, the large-scale circulation patterns consistently show a strong link with the annual NEE, and provide the potential as predictors for forest NEE at the three sites. All summer global climate indices are not significantly related to the

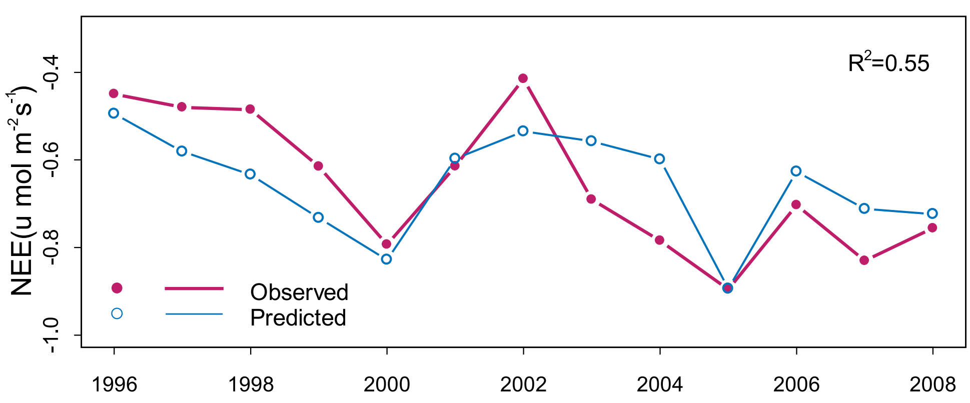

Figure 5. Observed and predicted annual net ecosystem exchange (NEE) at Howland Forest.

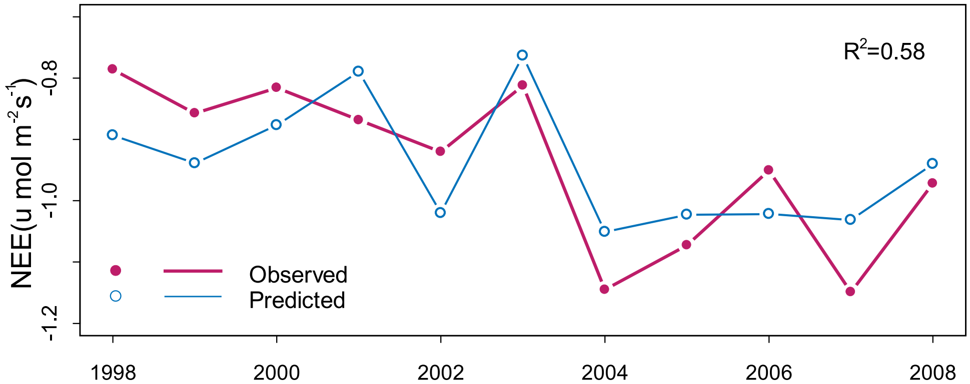

Figure 6. Observed and predicted annual net ecosystem exchange (NEE) at Morgan Monroe State Forest.

annual NEE at the three sites. In addition, the annual NEE at the three sites is all inversely correlated with the AMO.

[28] Except for the AMO, the annual NEE at the three sites are linked to other different global climate indices. Several reasons may be responsible for the differences. The large-scale circulation patterns have different effects on climate at the three sites due to their different geographic location (Table 1), and CO_2 exchange responds differentially with respect to latitude and climatic variations [e.g., *Nemani et al.*, 2003; *Gong and Ho*, 2003; *Notaro et al.*, 2006a; *Hember and Lafleur*, 2008; *Grant et al.*, 2009; *Wharton et al.*, 2009]. Another possible reason is that the three AmeriFlux research sites have different forest composition species, which affects the response of CO_2 exchange to the climate [e.g., *Hadley et al.*, 2009; *Richardson et al.*, 2009]. In this study, the annual NEE of deciduous-dominated Harvard Forest and Morgan Monroe State Forest exhibits significant correlations with climate indices in fall, while conifer-dominated Howland Forest NEE is closely linked to climate indices in winter and spring. Other characteristics of sites such as hydrological conditions, topography, disturbance, nutrient, and measurement errors may also introduce some differences [*Hember and Lafleur*, 2008; *Grant et al.*, 2009; *Hadley et al.*, 2009]. Moreover, the study periods for the three sites are different, but in all cases, the data length is short. The short data length implies that the uncertainty may be relatively large, so our results are subject to the study period.

4. Conclusions

[29] Long-term measurements (1992–2007) of CO_2 flux at Harvard Forest provide an excellent opportunity to investigate the responses of this ecosystem to large-scale circulation patterns. Using spearman's rank correlation and composite analysis, the relationships between the annual CO_2 exchange variations and large-scale circulation patterns are identified. We find that the annual GEE is significantly related with the fall AMO, the winter EP-NP, the spring MEI and PDO. The annual NEE shows strong links with the fall AMO and PDO, and the annual R is associated with the fall MEI and PNA.

[30] We further discuss possible physical processes responsible for the global climate indices– CO_2 exchange links. The regional circulation patterns are found to be closely related to global climate indices which show robust relationships with the GEE, NEE, and R at Harvard Forest. Surface climate factors including precipitation, temperature, and radiation determine interannual variability of the annual CO_2 exchange in the forest. We suggest that changes in large-scale patterns, through modification of regional circulation features over the northeast United States, can influence one or more surface climatic factors. Due to the relatively short observational record, the statistical significance cannot always be judged at the 95% confidence level. Further investigations are clearly needed to clarify the uncertainties and the related physical mechanisms.

[31] Regressions based on these climate indices are developed to simulate the annual GEE, NEE and R. However, the four climate indices associated with annual GEE are highly correlated to each other, and the two indices associated with the annual R also exhibit high degree of correlation. Therefore, instead of regressing highly correlated climate indices directly, we compute two new indices (CI_{GEE} and CI_R) based on their linear combination to avoid the problems of multicollinearity. The two new indices can account for 41% and 27% of the total variance in the annual GEE and R, respectively. On the other hand, the fall AMO and PDO contribute to 40% of the total variance in the annual NEE. The methodology is further applied to other two AmeriFlux sites that both have more than 10 years of CO_2 flux records available. The global climate indices are found to make a dominant contribution to the interannual NEE variability at the two sites. The results together with that of Harvard Forest suggest that the global climate indices have the potential as predictors for northern midlatitude forest CO_2 exchange.

[32] **Acknowledgments.** We would like to thank the following principal investigators for their hard work and dedication to collection and archiving of these data: J. William Munger and Steven Wofsy (Harvard Forest), David Hollinger (Howland Forest), and Danilo Dragoni (Morgan Monroe State Forest). We are also grateful to two anonymous reviewers, whose insightful comments and constructive criticism help to significantly improve the paper. The work was supported by the "100-talent program" of the Chinese Academy of Sciences, the special fund for President's prize of the Chinese Academy of Sciences, and National Basic Research Program (2009CB21405).

References

Aber, J. D., W. H. McDowell, K. J. Nadelhoffer, A. Magill, G. Berntson, M. Kamakea, S. G. McNulty, W. Currie, L. Rustad, and I. Fernandez

(1998), Nitrogen saturation in temperate forest ecosystems: Hypotheses revisited, *BioScience*, *48*, 921–934, doi:10.2307/1313296.
Albani, M., et al. (2006), The contributions of land-use change, CO_2 fertilization, and climate variability to the Eastern US carbon sink, *Global Change Biol.*, *12*, 2370–2390, doi:10.1111/j.1365-2486.2006.01254.x.
Baldocchi, D. D. (2003), Assessing the eddy-covariance technique for evaluating the carbon dioxide exchange rates of ecosystems: Past, present and future, *Global Change Biol.*, *9*, 479–492, doi:10.1046/j.1365-2486.2003.00629.x.
Barford, C. C., et al. (2001), Factors controlling long- and short-term sequestration of atmospheric CO_2 in a mid-latitude Forest, *Science*, *294*, 1688–1691, doi:10.1126/science.1062962.
Barnston, A. G., and R. E. Livezey (1987), Classification, seasonality and persistence of low-frequency atmospheric circulation patterns, *Mon. Weather Rev.*, *115*, 1083–1126, doi:10.1175/1520-0493(1987)115<1083:CSAPOL>2.0.CO;2.
Battle, M., M. L. Bender, P. P. Tans, J. W. C. White, J. T. Ellis, T. Conway, and R. J. Francey (2000), Global carbon sinks and their variability inferred from atmospheric O_2 and $\delta^{13}C$, *Science*, *287*, 2467–2470, doi:10.1126/science.287.5462.2467.
Bell, G. D., and J. E. Janowiak (1995), Atmospheric circulation associated with the Midwest floods of 1993, *Bull. Am. Meteorol. Soc.*, *76*, 681–695, doi:10.1175/1520-0477(1995)076<0681:ACAWTM>2.0.CO;2.
Boisvenue, C., and S. W. Running (2006), Impacts of climate change on natural forest productivity-evidence since the middle of the 20th century, *Global Change Biol.*, *12*, 862–882, doi:10.1111/j.1365-2486.2006.01134.x.
Bradbury, J. A., B. D. Keim, and C. P. Wake (2002), U.S. east coast trough indices at 500 hPa and New England winter climate variability, *J. Clim.*, *15*, 3509–3517, doi:10.1175/1520-0442(2002)015<3509:USECTI>2.0.CO;2.
Budikova, D. (2005), Impact of the Pacific Decadal Oscillation on relationships between temperature and the Arctic Oscillation in the USA in winter, *Clim. Res.*, *29*, 199–208, doi:10.3354/cr029199.
Caspersen, J., et al. (2000), Contributions of land-use history and enhanced tree growth to carbon accumulation in US forests, *Science*, *290*, 1148–1151, doi:10.1126/science.290.5494.1148.
Churkina, G., D. Schimel, B. H. Braswell, and X. M. Xiao (2005), Spatial analysis of growing season length control over net ecosystem exchange, *Global Change Biol.*, *11*, 1777–1787, doi:10.1111/j.1365-2486.2005.001012.x.
Dunn, A. L., C. C. Barford, S. C. Wofsy, M. L. Goulden, and B. C. Daube (2007), A long-term record of carbon exchange in a boreal black spruce forest: Means, responses to interannual variability, and decadal trends, *Global Change Biol.*, *13*, 577–590, doi:10.1111/j.1365-2486.2006.01221.x.
Enfield, D. B., A. M. Mestas-Nuñez, and P. J. Trimble (2001), The Atlantic Multidecadal Oscillation and its relation to rainfall and river flows in the continental U.S., *Geophys. Res. Lett.*, *28*, 2077–2080, doi:10.1029/2000GL012745.
Freedman, J. M., D. R. Fitzjarrald, K. E. Moore, and R. K. Sakai (2001), Boundary layer clouds and vegetation-atmosphere feedbacks, *J. Clim.*, *14*, 180–197, doi:10.1175/1520-0442(2001)013<0180:BLCAVA>2.0.CO;2.
Frontier, S. (1976), Study of the decrease of eigenvalues in principal component analysis: Comparison with the broken stick model, *J. Exp. Mar. Biol. Ecol.*, *25*, 67–75, doi:10.1016/0022-0981(76)90076-9.
Goldstein, A., et al. (2000), Effects of climate variability on the carbon dioxide, water and sensible heat fluxes above a ponderosa plantation in the Sierra Nevada (CA), *Agric. For. Meteorol.*, *101*, 113–129, doi:10.1016/S0168-1923(99)00168-9.
Gong, D.-Y., and C.-H. Ho (2003), Detection of large-scale climate signals in spring vegetation index (normalized difference vegetation index) over the Northern Hemisphere, *J. Geophys. Res.*, *108*(D16), 4498, doi:10.1029/2002JD002300.
Goulden, M. L., J. W. Munger, S. M. Fan, B. C. Daube, and S. C. Wofsy (1996), Effects of interannual climate variability on the carbon dioxide exchange of a temperate deciduous forest, *Science*, *271*, 1576–1578, doi:10.1126/science.271.5255.1576.
Grant, R. F., A. G. Barr, T. A. Black, H. A. Margolis, A. L. Dunn, J. Metsaranta, S. Wang, J. H. McCaughey, and C. A. Bourque (2009), Interannual variation in net ecosystem productivity of Canadian forests as affected by regional weather patterns—A Fluxnet-Canada synthesis, *Agric. For. Meteorol.*, *149*, 2022–2039, doi:10.1016/j.agrformet.2009.07.010.
Graumlich, L. J., L. B. Brubaker, and C. C. Grier (1989), Long-term trends in forest net primary productivity—Cascade Mountains, Washington, *Ecology*, *70*, 405–410, doi:10.2307/1937545.
Griffiths, M., and R. S. Bradley (2007), Variations of twentieth-century temperature and precipitation extreme indicators in the northeast United States, *J. Clim.*, *20*, 5401–5417, doi:10.1175/2007JCLI1594.1.
Hadley, J. L., J. O'Keefe, J. W. Munger, D. Y. Hollinger, and A. D. Richardson (2009), Phenology of forest-atmosphere carbon exchange for deciduous and coniferous forests in southern and northern New England: Variation with latitude and landscape position, in *Phenology of Ecosystem Processes*, pp. 119–141, Springer, New York, doi:10.1007/978-1-4419-0026-5_5.
Hanson, P., et al. (2004), Oak forest carbon and water simulations: Model intercomparisons and evaluations against independent data, *Ecol. Monogr.*, *74*, 443–489, doi:10.1890/03-4049.
Hember, R., and P. Lafleur (2008), Effects of serial dependence and large-scale tropospheric circulation on midlatitude North American terrestrial carbon dioxide exchange, *J. Clim.*, *21*, 751–770, doi:10.1175/2007JCLI1718.1.
Hollinger, D. Y., S. M. Goltz, E. A. Davidson, J. T. Lee, K. Tu, and H. T. Valentine (1999), Seasonal patterns and environmental control of carbon dioxide and water vapour exchange in an ecotonal boreal forest, *Global Change Biol.*, *5*, 891–902, doi:10.1046/j.1365-2486.1999.00281.x.
Hollinger, D. Y., et al. (2004), Spatial and temporal variability in forest-atmosphere CO_2 exchange, *Global Change Biol.*, *10*, 1689–1706, doi:10.1111/j.1365-2486.2004.00847.x.
Holton, J. R., and R. S. Lindzen (1972), An updated theory for the Quasi-Biennial cycle of the tropical stratosphere, *J. Atmos. Sci.*, *29*, 1076–1080, doi:10.1175/1520-0469(1972)029<1076:AUTFTQ>2.0.CO;2.
Houghton, R. A. (2000), Interannual variability in the global carbon cycle, *J. Geophys. Res.*, *105*(D15), 20,121–20,130, doi:10.1029/2000JD900041.
Houghton, R. A., J. L. Hackler, and K. T. Lawrence (1999), The US carbon budget: Contributions from land-use change, *Science*, *285*, 574–578, doi:10.1126/science.285.5427.574.
Hui, D., Y. Luo, and G. Katul (2003), Partitioning interannual variability in net ecosystem exchange between climatic variability and functional change, *Tree Physiol.*, *23*, 433–442.
Hurrell, J. W. (1995), Decadal trends in the North Atlantic Oscillation: Regional temperatures and precipitation, *Science*, *269*, 676–679, doi:10.1126/science.269.5224.676.
Hurrell, J. W. (1996), Influence of variations in extratropical wintertime teleconnections on Northern Hemisphere temperature, *Geophys. Res. Lett.*, *23*, 665–668, doi:10.1029/96GL00459.
Jackson, D. A. (1993), Stopping rules in principal components analysis: A comparison of heuristical and statistical approaches, *Ecology*, *74*, 2204–2214, doi:10.2307/1939574.
Keeling, R. F., C. P. Stephen, and M. Heimann (1996), Global and hemispheric CO_2 sinks deduced from changes in atmospheric CO_2 concentration, *Nature*, *381*, 218–221, doi:10.1038/381218a0.
Kunkel, E. K., et al. (2009), Trends in twentieth-century U.S. extreme snowfall seasons, *J. Clim.*, *22*, 6204–6216, doi:10.1175/2009JCLI2631.1.
Kutner, M. H., C. J. Nachtsheim, and J. Neter (2004), *Applied Linear Regression Models*, 701 pp., McGraw-Hill, New York.
Law, B. E. (2006), Carbon dynamics in response to climate and disturbance: Recent progress from multiscale measurements and modeling in AmeriFlux, in *Plant Responses to Air Pollution and Global Change*, edited by K. Omasa, I. Nouchi, and L. J. De Kok, pp. 205–213, Springer, Tokyo.
Leathers, D. J., B. Yarnal, and M. A. Palecki (1991), The Pacific/North American teleconnection pattern and United States climate. Part I: Regional temperature and precipitation associations, *J. Clim.*, *4*, 517–528, doi:10.1175/1520-0442(1991)004<0517:TPATPA>2.0.CO;2.
Legendre, P., and L. Legendre (1998), *Numerical Ecology*, 2nd Engl. ed., Elsevier, New York.
Mantua, N., S. Hare, Y. Zhang, J. M. Wallace, and R. Francis (1997), A Pacific interdecadal climate oscillation with impacts on salmon production, *Bull. Am. Meteorol. Soc.*, *78*, 1069–1079, doi:10.1175/1520-0477(1997)078<1069:APICOW>2.0.CO;2.
McCabe, G. J., M. A. Palecki, and J. L. Betancourt (2004), Pacific and Atlantic ocean influences on multidecadal drought frequency in the United States, *Proc. Natl. Acad. Sci. U. S. A.*, *101*, 4136–4141, doi:10.1073/pnas.0306738101.
Morgenstern, K., et al. (2004), Sensitivity and uncertainty of the carbon balance of Pacific Northwest Douglas-fir forest during an El Niño–La Niña cycle, *Agric. For. Meteorol.*, *123*, 201–219, doi:10.1016/j.agrformet.2003.12.003.
Munger, J. W. (2009), 20 years of NEE measurements at the Harvard Forest Environmental Measurement Site, paper presented at Harvard Forest Symposium-2009, Harvard Univ., Cambridge, Mass. (Available at http://harvardforest.fas.harvard.edu/asp/hf/symposium/showsymposium.html?id=745&year=2009)
Nemani, R. R., C. D. Keeling, H. Hashimoto, W. M. Jolly, S. C. Piper, C. J. Tucker, R. B. Myneni, and S. W. Running (2003), Climate-driven increases in global terrestrial net primary production from 1982 to 1999, *Science*, *300*, 1560–1563, doi:10.1126/science.1082750.
Notaro, M., W. C. Wang, and W. Gong (2006a), Model and observational analysis of the Northeast US regional climate and its relationship to the PNA and NAO patterns during early winter, *Mon. Weather Rev.*, *134*, 3479–3505, doi:10.1175/MWR3234.1.

Notaro, M., Z. Liu, and J. W. Williams (2006b), Observed vegetation-climate feedbacks in the United States, *J. Clim.*, *19*, 763–786, doi:10.1175/JCLI3657.1.
Ollinger, S. V., et al. (2008a), Canopy nitrogen, carbon assimilation, and albedo in temperature and boreal forests: Functional relations and potential climate feedbacks, *Proc. Natl. Acad. Sci. U. S. A.*, *109*, 19,335–19,340.
Ollinger, S. V., C. L. Goodale, K. Hayhoe, and J. P. Jenkins (2008b), Potential effects of climate change and rising CO_2 on ecosystem processes in northeastern U.S. forests, *Mitig. Adapt. Strategies Global Change*, *13*, 467–485, doi:10.1007/s11027-007-9128-z.
Peres-Neto, P. R., D. A. Jackson, and K. M. Somers (2003), Giving meaningful interpretation to ordination axes assessing loading significance in principal component analysis, *Ecology*, *84*, 2347–2363, doi:10.1890/00-0634.
Piao, S. L., et al. (2008), Net carbon dioxide losses of northern ecosystems in response to autumn warming, *Nature*, *451*, 49–52, doi:10.1038/nature06444.
Richardson, A. D., D. Y. Hollinger, J. D. Aber, S. V. Ollinger, and B. H. Braswell (2007), Environmental variation is directly responsible for short-but not long-term variation in forest-atmosphere carbon exchange, *Global Change Biol.*, *13*, 788–803, doi:10.1111/j.1365-2486.2007.01330.x.
Richardson, A. D., D. Y. Hollinger, D. B. Dail, J. T. Lee, J. W. Munger, and J. O'Keefe (2009), Influence of spring phenology on seasonal and annual carbon balance in two contrasting New England forests, *Tree Physiol.*, *29*, 321–331, doi:10.1093/treephys/tpn040.
Richman, M. B., P. J. Lamb, and J. R. Angel (1991), Relationships between monthly precipitation over central and eastern North America and the Southern Oscillation, paper presented at Fifth Conference on Climate Variations, Am. Meteorol. Soc., Denver, Colo.
Ropelewski, C., and M. Halpert (1986), North American precipitation and temperature patterns associated with the El Niño/Southern Oscillation (ENSO), *Mon. Weather Rev.*, *114*, 2352–2362, doi:10.1175/1520-0493(1986)114<2352:NAPATP>2.0.CO;2.
Schimel, D. S., et al. (2000), Contribution of increasing CO_2 and climate to carbon storage by ecosystems in the United States, *Science*, *287*, 2004–2006, doi:10.1126/science.287.5460.2004.
Schimel, D. S., et al. (2001), Recent patterns and mechanisms of carbon exchange by terrestrial ecosystems, *Nature*, *414*, 169–172, doi:10.1038/35102500.
Schmid, H. P., C. S. B. Grimmond, F. Cropley, B. Offerle, and H.-B. Su (2000), Measurements of CO_2 and energy fluxes over a mixed hardwood forest in the mid-western United States, *Agric. For. Meteorol.*, *103*, 357–374, doi:10.1016/S0168-1923(00)00140-4.
Siqueira, M. B., et al. (2006), Multiscale model intercomparisons of CO_2 and H_2O exchange rates in a maturing southeastern U.S. pine forest, *Global Change Biol.*, *12*, 1189–1207, doi:10.1111/j.1365-2486.2006.01158.x.
Sobolowski, S., and A. Frei (2007), Lagged relationships between North American snow mass and atmospheric teleconnection indices, *Int. J. Climatol.*, *27*, 221–231, doi:10.1002/joc.1395.
Tans, P. P., I. Y. Fung, and T. Takahashi (1990), Observational contrains on the global atmospheric CO_2 budget, *Science*, *247*, 1431–1438, doi:10.1126/science.247.4949.1431.
Thompson, D. W. J., and J. M. Wallace (1998), The Arctic Oscillation signature in the wintertime geopotential height and temperature fields, *Geophys. Res. Lett.*, *25*, 1297–1300, doi:10.1029/98GL00950.
Thompson, D. W. J., M. P. Baldwin, and J. M. Wallace (2002), Stratospheric connection to Northern Hemisphere wintertime weather: Implications for prediction, *J. Clim.*, *15*, 1421–1428, doi:10.1175/1520-0442(2002)015<1421:SCTNHW>2.0.CO;2.
Urbanski, S., C. Barford, S. Wofsy, C. Kucharik, E. Pyle, J. Budney, K. McKain, D. Fitzjarrald, M. Czikowsky, and J. W. Munger (2007), Factors controlling CO_2 exchange on timescales from hourly to decadal at Harvard Forest, *J. Geophys. Res.*, *112*, G02020, doi:10.1029/2006JG000293.
Wallace, J. M., and D. S. Gutzler (1981), Teleconnections in the geopotential height field during the North Hemispheric winter, *Mon. Weather Rev.*, *109*, 784–812, doi:10.1175/1520-0493(1981)109<0784:TITGHF>2.0.CO;2.
Wang, K., R. E. Dickinson, and S. Liang (2008), Observational evidence on the effects of clouds and aerosols on net ecosystem exchange and evapotranspiration, *Geophys. Res. Lett.*, *35*, L10401, doi:10.1029/2008GL034167.
Wharton, S., L. Chaemer, M. Falk, and K. T. Paw U (2009), Strong links between teleconnections and ecosystem exchange found at a Pacific Northwest old-growth forest from flux tower and MODIS EVI data, *Global Change Biol.*, *15*, 2187–2205, doi:10.1111/j.1365-2486.2009.01952.x.
Wofsy, S. C., et al. (1993), Net exchange of CO_2 in a mid-latitude forest, *Science*, *260*, 1314–1317, doi:10.1126/science.260.5112.1314.
Wolter, K., and M. S. Timlin (1993), Monitoring ENSO in COADS with a seasonally adjusted principal component index, paper presented at 17th Climate Diagnostics Workshop, NSSL, Norman, Okla.
Wolter, K., and M. S. Timlin (1998), Measuring the strength of ENSO events: How does 1997/1998 rank?, *Weather*, *53*, 315–324.
Xiao, X. M., D. Hollinger, J. Aber, M. Goltz, E. A. Davidson, Q. Y. Zhang, and B. Moore III (2004), Satellite-based modeling of gross primary production in an evergreen needleleaf forest, *Remote Sens. Environ.*, *89*, 519–534, doi:10.1016/j.rse.2003.11.008.
Zhang, J., W.-C. Wang, and L. R. Leung (2008), Contribution of land-atmosphere coupling to summer climate variability over the contiguous United States, *J. Geophys. Res.*, *113*, D22109, doi:10.1029/2008JD010136.
Zhou, L. M., C. J. Tucker, R. K. Kaufmann, D. Slayback, N. V. Shabanov, and R. B. Myneni (2001), Variations in northern vegetation activity inferred from satellite data of vegetation index during 1981 to 1999, *J. Geophys. Res.*, *106*(D17), 20,069–20,083, doi:10.1029/2000JD000115.

G. Huang, RCE-TEA and LASG, Institute of Atmospheric Physics, Chinese Academy of Sciences, Beijing 100029, China.
M. Notaro, Center for Climatic Research, University of Wisconsin-Madison, Madison, WI 53706, USA.
L. Wu and J. Zhang, Center for Monsoon System Research, Institute of Atmospheric Physics, Chinese Academy of Sciences, Beijing 100029, China. (zjy@mail.iap.ac.cn)